Journal of Hydrology 615 (2022) 128578

Contents lists available at ScienceDirect

Journal of Hydrology

journal homepage: www.elsevier.com/locate/jhydrol

Research papers

The effect of natural and engineered hydraulic conditions on river-floodplain connectivity using hydrodynamic modeling and particle tracking analysis

Yang Xiao [a,b,c,d,*], Jiaming Liu [a,c,d], Carlo Gualtieri [e], Jun Fu [c], Ran Gu [c], Zixuan Wang [c], Taotao Zhang [d], Jian Zhou [a,c]

[a] State Key Laboratory of Hydrology, Water Resources and Hydraulic Engineering, Hohai University, Nanjing, China
[b] Yangtze Institute for Conservation and Development, Hohai University, Nanjing, China
[c] College of Water Conservancy and Hydropower Engineering, Hohai University, Nanjing, China
[d] Institute of Water Science and Technology, Hohai University, Nanjing, China
[e] Department of Structures for Engineering and Architecture, University of Napoli Federico II, Italy

ARTICLE INFO

This manuscript was handled by marco borga, Editor-in-Chief, with the assistance of George Constantinescu, Associate Editor

Keywords:
River-floodplain connectivity
Hydrodynamic modeling
Particle tracking
Natural floods
Engineered hydraulic conditions

ABSTRACT

Hydraulic conditions and water resources management projects can significantly alter river-floodplain connectivity, which in turn can alter hydrologic and biogeochemical processes in river corridors. In this study, the hydrodynamics of river-floodplain connectivity under different flood conditions and the effect of the Nanchang Water Resources Project Group (NWRPG) in the middle branch of the Ganjang River were investigated using a combination of two-dimensional hydrodynamic simulations and particle tracking. The hydrodynamic model was calibrated and validated using data from several gauging stations and field measurements. Floods in the Ganjang River can be limited to the river itself ("River Flood", flood with normal lake level) or further extended to the Poyang Lake ("Lake Flood", flood with high lake level). The results show that compared with "River Flood" scenarios, "Lake Flood" scenarios increased the water level flooding a larger area. The flow velocity decreased and the residence time (RT) of particles increased. The particle travel distance (PTD) of "River Flood" was larger than that of "Lake Flood". The larger the flood, the greater the transboundary flux between the river and the floodplain, and the shorter the RT and PTD. The effect of NWRPG was the permanent flooding of part of the river floodplain, causing some habitat loss. Due to the increase in discharge, the implementation of the NWRPG results in a shorter RT with a smaller standard deviation, which has little effect on the PTD distribution. These findings can facilitate river connectivity restoration efforts in the Ganjang River and also provide a reference for assessing the impact of barrage projects.

1. Introduction

The compound cross-section rivers, comprised of a river's main channel and its floodplains, are the most common type of lowland river system (Rowiński and Radecki-Pawlik, 2015). River-floodplain connectivity is a typical part of hydrologic connectivity (Gooseff et al., 2017). During the dry season, water flow is limited to the main channel, while during flooding seasons, floodplains are filled by water performing important environmental (Mahl et al., 2015) and biological functions (Covino, 2017; Kang and Choi, 2005).

The interaction between the river channel and its floodplains has long been recognized as a key process in maintaining riverine ecosystems because it facilitates the exchange of large amounts of water, sediment or organic matter, and nutrients between rivers, floodplains, and riparian wetlands (Harvey and Gooseff, 2015; Shuai et al., 2017). Quantitative analysis of hydrologic connectivity between rivers and their floodplains in response to different hydrological conditions and to the implementation of water resources management projects is important to identify how the river-floodplain connectivity could affect water quality and ecological processes in river systems (Fu et al., 2020; Tan et al., 2021). The lateral exchange of water, sediment, nutrients, and contaminants between a river and its floodplain is dependent on

* Corresponding author at: College of Water Conservancy and Hydropower Engineering, Hohai University, Nanjing, China.
E-mail address: Sediment_lab@hhu.edu.cn (Y. Xiao).

https://doi.org/10.1016/j.jhydrol.2022.128578
Received 18 May 2022; Received in revised form 15 August 2022; Accepted 4 October 2022
Available online 12 November 2022

hydrodynamics and river morphology. Water resources management projects could drastically modify the hydrological conditions and impact the rivers' hydrodynamics, sediment transport, and morphology.

In a compound channel, momentum exchange occurs at the interface between the rivers and the floodplains (Dupuis et al., 2017; Proust et al., 2017) due to the velocity difference between the main channel and the floodplains. At the interface between the floodplain and the main channel, Kelvin-Helmholtz (KH) instability causes a complex turbulent structure related to a series of vertically orientated vortices and streamwise orientated vortices located both in the floodplain and the main channel (Proust and Nikora, 2020). Spiral vortices (Lai et al., 2008) and coherent structures of various time and length scales (Xiao and Wang, 2007) are observed. Past studies on compound channels (Ding et al., 2022; Knight and Demetriou, 1983; Shiono and Knight, 1991), focused on the impact of changes in the depth ratio and floodplain characteristics on hydrodynamic properties such as flow velocity distribution, turbulent flow structure, and boundary shear stress.

Because investigating river-floodplain connections during flooding conditions is extremely dangerous for instrumentation and researchers, river-floodplain interaction field studies are uncommon. Models based upon the shallow-water equations are widely used on large scale free surface flow problems (Tan et al., 2021). Particle tracking methods have proven to be effective in delineating flow fields (Wang et al., 2018), determining flow paths (Li et al., 2008) and travel times (Jing et al., 2021). These methods have also been used to study pollutant dispersion (Salamon et al., 2006), sediment transport (Zhao et al., 2011), oil spills (Goeury, 2012), algal movement (Joly, 2011) and connectivity patterns in the northern Gulf of California (Marinone et al., 2008). Chen et al. (2020) first proposed the use of a particle-tracking simulation method to quantify flow dynamics between a river channel and its floodplains. Particle tracking methods are also able to figure out the water travel length and residence time inside the floodplains. Lowland rivers are often located in areas with a large population, in which the conservation of good water quality levels is challenging. This leads to the creation of projects to manage water resources, which may change the way rivers and floodplains connect.

Using hydrodynamic modeling and particle tracking analysis, the present study investigates the hydrological connectivity of river-floodplain systems under changing natural and engineered hydraulic conditions. The Ganjiang River is the largest tributary of the Poyang Lake Basin and the fourth largest tributary of the Yangtze River. It flows from south to north through the entire territory of Jiangxi Province, China. The management of the Ganjiang River is crucial to the hydrology and ecology of the Poyang Lake Basin and even of the Yangtze River Basin. To raise the water level during the low flow season, the Nanchang Water Resources Project Group (NWRPG) is being planned. The main scientific objectives addressed in this study are to:

analyze the characteristics of river-floodplain interactions under different flood characteristics;
evaluate the impact of the implementation of the NWRPG on river-floodplain connectivity.

2. Method

2.1. Study site: The lower middle branch of Ganjiang river

The study was conducted at the lower middle branch of the Ganjiang River in Jiangxi, China. The Ganjiang River flows north through the western part of Jiangxi Province before entering Poyang Lake and, later, the Yangtze River (Fig. 1 a). This river provides water resources to the city of Nanchang as well as acts as an ecological corridor for fish and other aquatic species. Floods in the Ganjiang River can be generally divided into two types: "River Flood" and "Lake Flood". They have a different frequency. The "River Flood" refers to the flood in the Ganjiang River but not in the Poyang Lake. The "Lake Flood" means both the Ganjiang River, and the Poyang Lake are under flood conditions. However, due to uncontrolled river sand mining, the low flow water level in the lower Ganjiang River is lower than before. Water utilization conditions have deteriorated, and the water resources for urban water supply

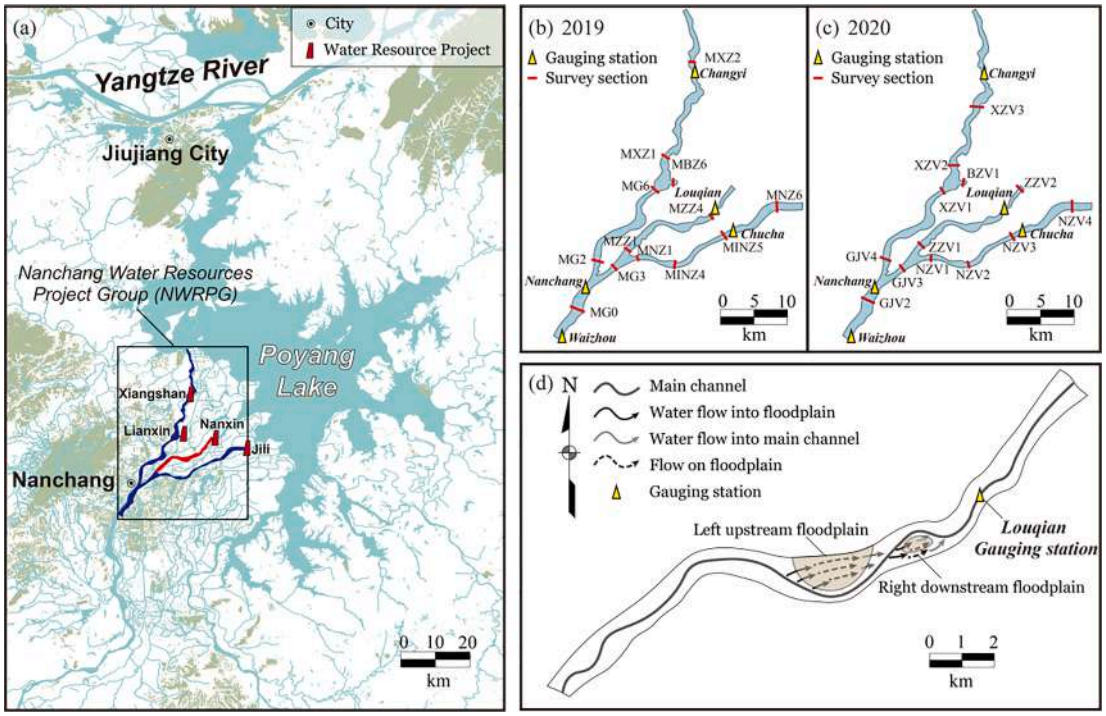

Fig. 1. (a) Map of the Ganjiang River, the red trapezoids are the NWRPG; (b) the validation model area, the yellow triangles are the gauging stations, the red lines are the survey sections in 2019; (c) the survey sections in 2020; (d) the study site the lower middle branch of Ganjiang River. Illustrated in (d) is the entire river reach for flood simulation. Arrows that illustrating the flow exchange behaviors are sketched based upon the flow vectors.

and agricultural irrigation in the region are scarce. In recent years, several water resources management projects, such as for flood control, waterway management, and environmental management, have been implemented or planned in the Ganjiang River Basin (Liu, 2018). The Nanchang Water Resources Project Group (NWRPG) is being planned with four individual projects to raise the water level in the downstream Ganjiang River during the low flow season (the Xiangshan Project, the Lianxin Project, the Nanxin Project, and the Jili Project; see Fig. 1a for the positions of the corresponding projects). The main hydraulic structures used in the NWRPG include gates, ship locks, and fish tunnels, etc. From April to July (i.e., the flood season), the gates will be fully open; from August to March of the following year, the river level will be controlled. After the completion of these projects, it is anticipated that the water level will rise and the discharge will increase during the dry season, while the water level will remain stable during the flood season.

2.2. Governing equations for fluid flow and particle transport

The two-dimensional shallow water equations (SWEs) are implemented for hydrodynamic modeling because of their ability to accurately simulate surface hydraulics in river-floodplain systems. They have achieved widespread application in a variety of complex free-surface flows (Cao et al., 2020; He et al., 2018; Lim et al., 2019; Tang et al., 2020):

$$\frac{\partial h}{\partial t}+\boldsymbol{u}\cdot\nabla(h)+h\mathrm{div}(\boldsymbol{u})=S_h \tag{1}$$

$$\frac{\partial u}{\partial t}+\boldsymbol{u}\cdot\nabla(u)=-g\frac{\partial Z}{\partial x}+S_x+\frac{1}{h}\mathrm{div}[h(\nu+\nu_t)\nabla u] \tag{2}$$

$$and\ \frac{\partial v}{\partial t}+\boldsymbol{u}\cdot\nabla(v)=-g\frac{\partial Z}{\partial y}+S_y+\frac{1}{h}\mathrm{div}[h(\nu+\nu_t)\nabla v]$$

where h is the water depth; t is the time, u and v are depth-integrated velocity components in the x- and y-directions, respectively; S_h is the source or sink of fluid; g is the gravity acceleration, Z is the free surface elevation; S_x and S_y are source terms that represent the bottom friction, the Coriolis force and the influence of wind; ν is the molecular viscosity. ν_t is the momentum diffusion coefficient (turbulent viscosity) which is estimated through the standard $k-\varepsilon$ turbulence model(Launder and Spalding, 1983):

$$\nu_t=C_\mu\frac{k^2}{\varepsilon} \tag{4}$$

where k is the turbulent kinetic energy; ε is the dissipation rate of turbulent energy; C_μ is a constant, experimentally found to be 0.09 (Launder et al., 1973; Rodi, 1972).

The quantities k and ε are obtained by solving the following depth-averaged two-dimensional transport equations (Rastogi and Rodi, 1978):

$$\frac{\partial k}{\partial t}+\boldsymbol{u}\cdot\nabla(k)=\frac{1}{h}\mathrm{div}\left(h\frac{\nu_t}{\sigma_k}\nabla k\right)+P-\varepsilon+P_{kv} \tag{5}$$

$$\frac{\partial \varepsilon}{\partial t}+\boldsymbol{u}\cdot\nabla(\varepsilon)=\frac{1}{h}\mathrm{div}\left(h\frac{\nu_t}{\sigma_\varepsilon}\nabla\varepsilon\right)+\frac{\varepsilon}{k}(c_{1\varepsilon}P-c_{2\varepsilon}\varepsilon)+P_{\varepsilon v} \tag{6}$$

where P is the production term, P_{kv} and $P_{\varepsilon v}$ are due to the shear force of flow along the vertical, $c_{1\varepsilon}$ is a constant being 1.44, $c_{2\varepsilon}$ is 1.92, σ_k is 1.0, σ_ε is 1.3 (Hervouet, 2007).

During the dry season, the flow in the Ganjiang River is limited inside the main channel having a curved planform. In a curved channel, the flow speeds up in the direction of the curve, and centrifugal forces act in proportion to the average speed (Blankaert et al., 2006). The development and decay processes of secondary flows in curved channels can be accounted for with the transport equation for streamwise vorticity (Bernard and Schneider, 1992; Wang and Tassi, 2014):

$$\frac{\partial\Omega}{\partial t}+u\frac{\partial\Omega}{\partial x}+v\frac{\partial\Omega}{\partial y}=\frac{A_s\sqrt{C_f}|u|^2}{Rh\left(1+\frac{9h^2}{R^2}\right)}-D_s\sqrt{C_f}\Omega\frac{|u|}{h}+\frac{1}{h}\nabla[(\nu+\nu_t)h\nabla\Omega] \tag{7}$$

where Ω is the streamwise vorticity, C_f is a friction coefficient, R is the local radius of curvature, A_s and D_s are empirical coefficients that determine the rate of vorticity production and dissipation, respectively. The solution of Equation (7) provides the streamwise stresses that result from the deviation of velocity from the depth-averaged velocity:

$$\tau_s=\rho h|\boldsymbol{u}|\Omega\sqrt{C_f} \tag{8}$$

where ρ is the water density. In a Cartesian coordinate system, the accelerations induced by secondary currents are computed as follows:

$$\boldsymbol{S}=(S_x,S_y)\approx\rho^{-1}\frac{\boldsymbol{u}}{|\boldsymbol{u}|}\left[\boldsymbol{n}\cdot\nabla(h\tau_s)+\frac{2h\tau_s}{R}\right] \tag{9}$$

where $\boldsymbol{n}$ is unit vector normal to the depth-averaged velocity vector $\boldsymbol{u}$. The term $\boldsymbol{n}\cdot\nabla(h\tau_s)$ can be written as:

$$\boldsymbol{n}\cdot\nabla(h\tau_s)=\frac{v(h\tau_s)_x-u(h\tau_s)_y}{|\boldsymbol{u}|} \tag{10}$$

and the local radius of curvature is determined by the expression:

$$R=\frac{|\boldsymbol{u}|^3}{uv(v_y-u_x)+u^2v_x-v^2u_x} \tag{11}$$

2.3. Particle tracking model

To better understand the details of flow dynamics, we conducted a two-dimensional Lagrangian particle tracking study to examine how flow parcels move through the study region. Here, we consider observations of passive particles transported by the river flow. The state of the flow is described in Eulerian coordinates by the shallow water equations. The link between the Lagrangian data and the classical Eulerian variables of the shallow water model is made by the following two-dimensional transport model:

$$\frac{d\boldsymbol{x}}{dt}=\boldsymbol{U}(\boldsymbol{x}(t),t) \tag{12}$$

where $\boldsymbol{x}$ is the coordinate vector of a particle as a function of time, $\boldsymbol{U}$ is the velocity vector at time t. Integrating (12) yields:

$$\boldsymbol{x}(t+\Delta t)=\boldsymbol{x}(t)+\int_t^{t+\Delta t}\boldsymbol{U}(\boldsymbol{x}(t),t)dt \tag{13}$$

The numerical integration was performed with a fourth-order Runge-Kutta algorithm:

$$a=U(\boldsymbol{x}_k,t)\Delta t \tag{14}$$

$$b=U(\boldsymbol{x}_k,a/2)\Delta t \tag{15}$$

$$c=U(\boldsymbol{x}_k,b/2)\Delta t \tag{16}$$

$$d=U(\boldsymbol{x}_k,c)\Delta t \tag{17}$$

$$\boldsymbol{x}(t+\Delta t)=\boldsymbol{x}(t)+(a+2b+2c+d)/6 \tag{18}$$

A MATLAB code that uses the fourth order of the Runge-Kutta method to track particles was prepared in-house. In a depth-averaged shallow water flow field, each 2-D particle emitted at a given horizontal plane point is associated with the scalar property flow depth, which corresponds to a vertical line or water column in the flow domain. Therefore, statistics for a large number of two-dimensional particles weighted by their flow depths are thus capable of representing the actual

dynamics of the water body in the two-dimensional plane. Integrating along the depth shows the properties of a two-dimensional particle that represents a body of water (Chen et al., 2020):

$$F_i = \int_0^h f_i dz \tag{19}$$

where i is the particle number, F is the property for a water column that can be calculated by integrating f along the depth of the column (e.g. F is the mass flux and f is the velocity magnitude).

Using the particle method, such a property can be expressed by:

$$F_i = \sum_{k=1}^{N_i} f_{i,j} H_{i,j} = h_i \bar{f}_i \tag{20}$$

where $f_{i,j}$ is the property f of the j th unit volume in the domain, $\bar{f}_i$ is the average value of the property f for the water column, $H_{i,j}$ is the height of the j th unit volume. This weighted analysis approach applies to the statistical properties of 2-D particles.

2.4. Boundary settings and equations solving

The boundary conditions for the numerical domain are set as steady flow, which are presented in Fig. 2b. On the upstream boundary, a specified discharge is prescribed, while the corresponding water level is assigned on the downstream boundary. The right or left boundary conditions (relative to the flow direction) of the model domain are considered no flow boundary conditions.

The system of partial differential equations represented in Eq. (1–11) was solved with TELEMAC-2D (a shallow water equations finite element model (FEM) solver of the integrated free-surface flow suite TELEMAC-MASCARET), which was developed initially by the National Hydraulics and Environment Laboratory (LNHE) of the Research and Development Directorate of the French Electricity Board (EDF R&D, France). A conjugate gradient method was used to solve the hydrodynamic propagation step and the standard $k-\varepsilon$ model system (Hervouet, 2007).

The Surface water Modeling System (SMS) was used for triangle mesh generation. After format conversion with Blue Kenue, Telemac2d can use the meshes generated by SMS. A higher density of elements was constructed in the vicinity of the main channel to obtain a more accurate solution (Fig. 2b). The model domain is ~ 21,000 m in length and 420 ~ 1250 m in width. A grid refinement was first conducted to ensure mesh independence of the results (Blocken and Gualtieri, 2012). Three meshes with element nodes of 4846, 6460, and 24,959 were generated, respectively. Table 1 compares the surface level and velocity of $P1$ (Fig. 2b). Results with a mesh of ~ 7000 nodes and above were mesh-independent. Finally, a mesh with 48,818 cells and 24,959 nodes was used to provide a more realistic flow structure and smooth particle trajectories. In the channel, the minimum element size was 25 m, and as this length gradually increased from channel to floodplain, the maximum size was 45 m.

Table 1
Grid size sensitivity analysis in hydraulic model.

Average grid size [m]	Node number [-]	Grid number [-]	Surface level [m]	Velocity magnitude [m/s]
58.9	4,846	9,121	15.36	0.17
50.8	6,460	12,280	15.35	0.19
25.5	24,959	48,818	15.33	0.17

The simulation was carried out over one year for a wider range of the river reach and included the upper part of the study area and other branches of the Ganjiang River to use the data from more gauging stations for validation (Fig. 2a). As shown in Fig. 1d, the left upstream floodplain is larger than the right downstream floodplain, and the downstream floodplain on the right was found to be permanently flooded after the implementation of the NWRPG in the subsequent study. Therefore, we conducted the particle tracking analysis in the area upstream of the left upstream floodplain.

Different hydrological conditions and different effects from the "River Flood", the "Lake Flood", and from the NWRPG were considered as scenarios (Table 1). According to the historical hydrological series, the average January runoff representing the dry season flow is 151.97 m^3/s, the annual average runoff is 491.168 m^3/s, and the 5 yr flood, 10 yr flood, and 20 yr flood discharges are 4,338.68, 4,898.08, and 5,338.53 m^3/s, respectively. The "River Flood" effects are considered for a 10 yr flood and 20 yr flood. The discharge is the same as in the "Lake Flood", while the water level is lower. Due to the implementation of NWRPG, the corresponding flows change at different frequencies. From the perspective of water resource availability, the dry season and average annual flows are lower than before, but water levels are higher. During the flood season, the water level is controlled at the same level as the "Lake Flood", but the discharge increases. The model scenarios are introduced for the setup of model scenarios (Table 2), and 12 runs were carried out. For each flood event, we released a total of 3,000 particles from the upstream section of the left upstream floodplain.

3. Results

3.1. Model calibration and validation

The 2013 hydrological data was used for model calibration. The model was calibrated by changing bed roughness, Manning coefficient (n). After validation, the manning coefficient was set to 0.024, which is

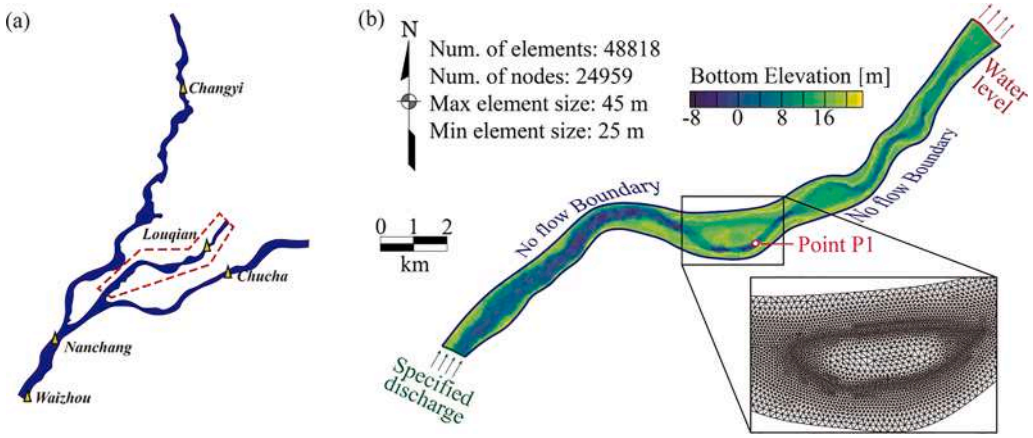

Fig. 2. (a) The model domain used for validation, and the distribution of gauging stations. (b)The boundary settings and the mesh of the modeling domain, the surface level and the velocity magnitude of point $P1$ was used in sensitivity analysis.

Table 2
Model scenarios of the numerical simulations.

	River Flood		Lake Flood		Implementation of NWRPG	
	Upstream Discharge [m^3/s]	Downstream Water Level [m]	Upstream Discharge [m^3/s]	Downstream Water Level [m]	Upstream Discharge [m^3/s]	Downstream Water Level [m]
January	–	–	151.97	12.87	122	15.49
Average	–	–	496.168	13.81	438	15.27
5 yr Flood	–	–	4338.68	19.65	5122.36	19.65
10 yr Flood	4898.08	17.45	4898.08	20.28	6037.04	20.28
20 yr Flood	5338.53	17.62	5338.53	20.78	6824.79	20.78

similar to the one used in the Poyang Lake model (Xiao et al., 2022). The trends of the numerical model and the measured water level in four gauging stations are basically consistent, the Nash coefficients are above 0.99, and the maximum water level error does not exceed 0.1 m (Fig. 3). The results show reasonable agreement between the model results and measured data.

For model validation, three hydrological tests were conducted in July 2019 (Waizhou discharge 3,780 m^3/s), September 2020 (Waizhou discharge 2,800 m^3/s) and October 2020 (Waizhou discharge 470 m^3/s) at thirteen survey sections (Fig. 1b and c). There are 12 or 13 measurement points available for each survey section. The cross-sectional average water levels and the vertically averaged streamwise velocity were measured. The hydrodynamic processes in July 2019 and September-October 2020 were calculated by the large model, and the results were compared with the measured cross-sectional average water levels and vertically averaged streamwise velocity (Fig. 4). Both the calculated water level and velocity show reasonable agreement with the measured data. The difference between the calculated and measured values of individual measurement points is mostly due to the time and topography of the tests.

3.2. Flood inundation and flow velocity distribution.

The map of the water depth and the flooded area, where gray indicates areas not flooded and color indicates the water depth of the inundation area, is presented in Fig. 5. In January scenarios, the flow passes in the main channel below the left upstream floodplain and in the upper and lower main channels of the right downstream floodplain (Fig. 5b1). The left upstream floodplain has some obvious isolated patches in January scenarios. These small wetland areas can play a vital role in preserving the ecological quality of rivers. At the average annual flow, the flow overflows the two main channels above and below the left floodplain, and the right downstream floodplain is mostly inundated (Fig. 5b2). The whole model domain is covered by water flow under the flood action of "Lake Flood" (Fig. 5 b3-5). Under the action of "River Flood", the left upstream floodplain still has partial outcropping (Fig. 5 a1-2), which could be a refuge for organisms. After the implementation of the NWRPG, water depth is increased for all conditions (Fig. 5 c). The main channel above the left upstream floodplain and the right downstream are always flooded. The river loses some of the upland areas that can be exposed during January.

The velocity field is displayed in Fig. 6. The implementation of the NWRPG reduces the velocity in January and the average annual flow (Fig. 6 c1-2). During floods, the main channel above the left upstream floodplain becomes the main overflow channel as the flood water tends to straighten out (Figs. 6 a1-2, b3-5, c3-5). Due to the much lower water level, the velocity under "River Flood" conditions is generally greater than under "Lake Flood" conditions (Fig. 6 a1-2). From the perspective of the January and average annual flow, the implementation of NWRPG results in increased water depth (Fig. 5 c1-2) and lower velocity (Fig. 6 c1-2). Due to the increased discharge in the middle branch under the NWRPG, the velocity becomes larger in the flood season (Fig. 6 c3-4).

3.3. Effect of the hydraulic conditions on lateral flow exchange

The transboundary flux is calculated by integrating unit discharge $\boldsymbol{uh}$ along riverbank lines:

$$q_{int} = \int \boldsymbol{uh}\cdot \mathrm{n} dl \tag{21}$$

where $\boldsymbol{u}$ is the velocity vector, h is the water depth, and n is the normal vector of bank line l pointing to the floodplain side.

Since the right downstream floodplain is permanently inundated, only the transboundary fluxes of the left upstream floodplain were analyzed in the present study. The transboundary flux of river-floodplain is presented in Fig. 7. The bank line of the left upstream floodplain is marked on Fig. 1d. The ratios of the transboundary fluxes to the upstream discharges are listed in Table 3. The total transboundary flux (total discharge from the river-floodplain boundary into or out of the river) is comparable to the upstream discharge, and the implementation of the NWRPG will cause all transboundary fluxes to rise (Fig. 7). This indicates that as the flow increases, the river-floodplain transboundary flux also increases. Under the average January discharge and average annual discharge, the transboundary fluxes and the ratio rise together. The ratios rise 3–17 times (Fig. 7 a). The connectivity of January was significantly enhanced. In contrast, during the

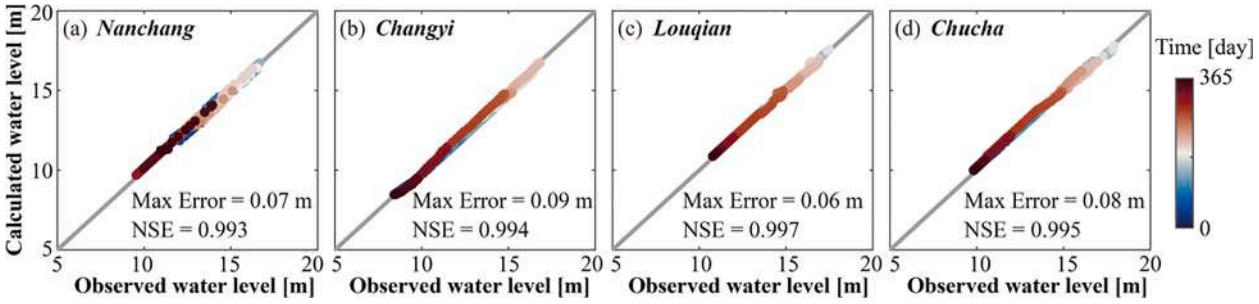

Fig. 3. Model results and water level measured by (a) Nanchang gauging station, (b) Changyi gauging station, (c) Louqian gauging station and (d) Chucha gauging station respectively.

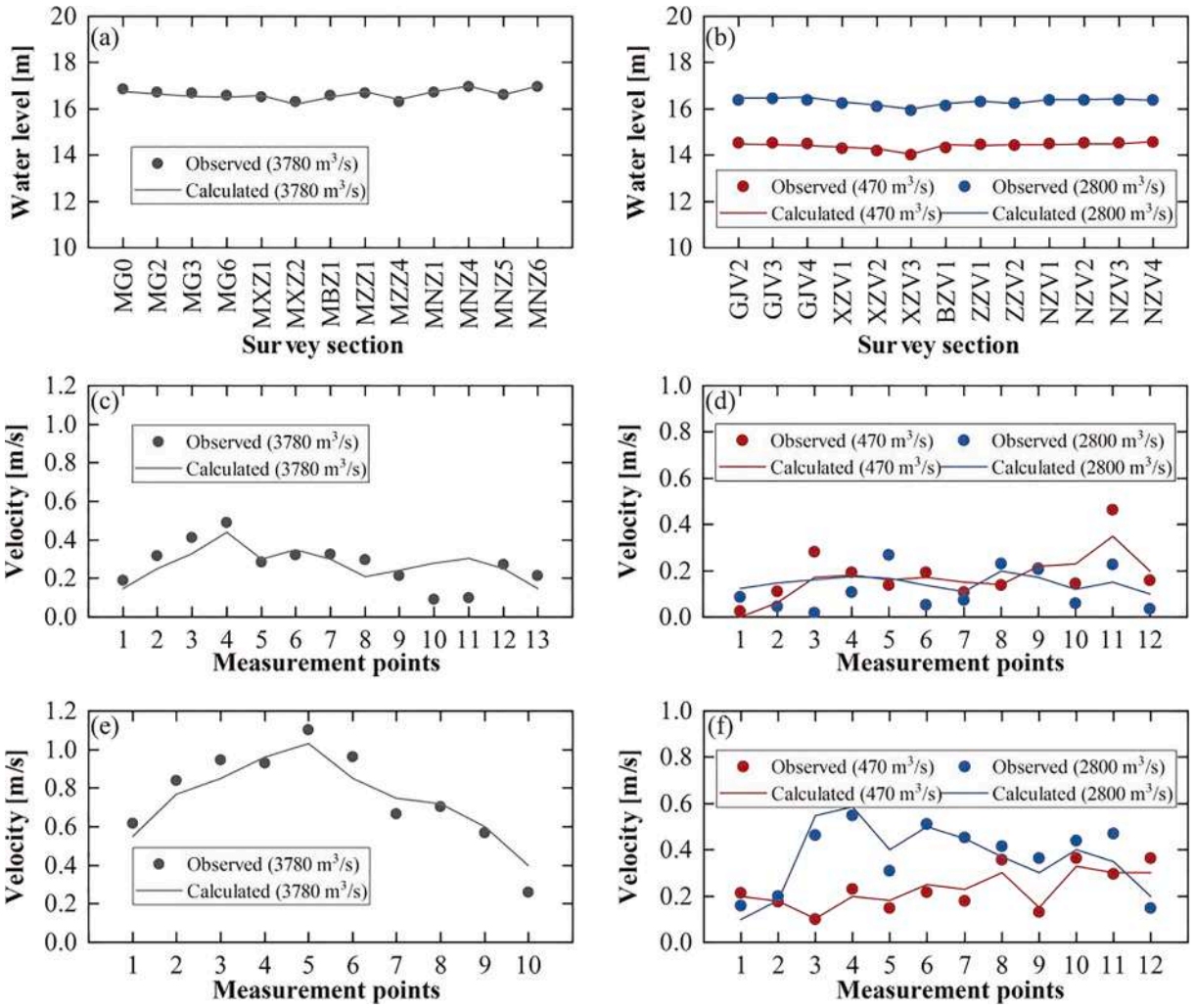

Fig. 4. Measured and modeled water level in (a) July 2019 and (b) September-October 2020. Measured and modeled velocity of (c) MZZ1 survey section in July 2019, (d) ZZV1 survey section in September-October 2020, (e) MZZ4 survey section in July 2019, (f) ZZV2 survey section in September-October 2020.

flood season, the transboundary fluxes, although rising, decline in proportion. In "River Flood" scenarios, the water level was lower and the water flow path is not as smooth and straight as in the "Lake Flood" scenarios. So, the transboundary flux and the ratio of "River Flood" are lower than both under "Lake Flood" and after the implementation of NWRPG.

3.4. Particles travel statistics in the river-floodplain system

The behavior of the deterministic particles is associated with the hydraulic conditions. Fig. 8 represents the particle movement under different hydraulic conditions. In January and under average annual discharge, the NWRPG considerably slowed down the movement of particles, which traveled a shorter distance during the same time interval (Figs. 8 b1-2, c1-2). During flood season, the discharge increased (Figs. 8 b3-5, c3-5) and the particles started to enter the river-floodplain interface at the mid-channel bar. Under such circumstances, the implementation of NWRPG will increase the discharge under every flood scenario and particles will travel a longer distance during the same time interval with respect to the pre-project situation (the particles in the region show a shorter time elapsed). In the meantime, there are significant increases in the number of particles passing through the floodplain. Under the "River Flood" scenarios, few particles passed over the mid-channel bar of the left upstream floodplain because that in-stream bar was only partially submerged (Fig. 5 a1-2) and the water didn't pass significantly over the mid-channel bar (Fig. 6 a1-2).

Additionally, the results of particle trajectory reveal certain critical aspects of the river-floodplain exchange dynamics. Together with the flow field (Fig. 6), the particle path lines (Fig. 8) demonstrate that particles mostly crossed the river-floodplain barrier at a relatively small angle, which shows that the river-floodplain exchange was mainly along the upstream and downstream directions, rather than through the lateral flow. This means that in this study, the river-floodplain exchange is determined by longitudinal flow connection and that the floodplain does not generally interact significantly with its immediate bordering stream reach, but rather with reaches upstream and downstream. This result is consistent with Chen et al. (2020), who did the particle analysis in a different curved compound channel. Both of our results show that in meandering compound channels, the main characteristics of the flood flow path are controlled by the shortest path of the overbank flow (a continuous line from upstream to downstream) and the main flood path no longer follows the main channel. The river-floodplain exchange in all flood scenarios was predominantly through the shortest flow path. The river-floodplain exchange in high water situations is predominantly through the straightened flow path.

Particle motions within the river-floodplain system are analyzed using the particle travel distance (PTD), which is the total distance traveled by a particle across the floodplain of a river reach (Chen et al., 2020), and the residence time (RT) of particles, which is the amount of time they spend in the floodplain (Defne and Ganju, 2015). These

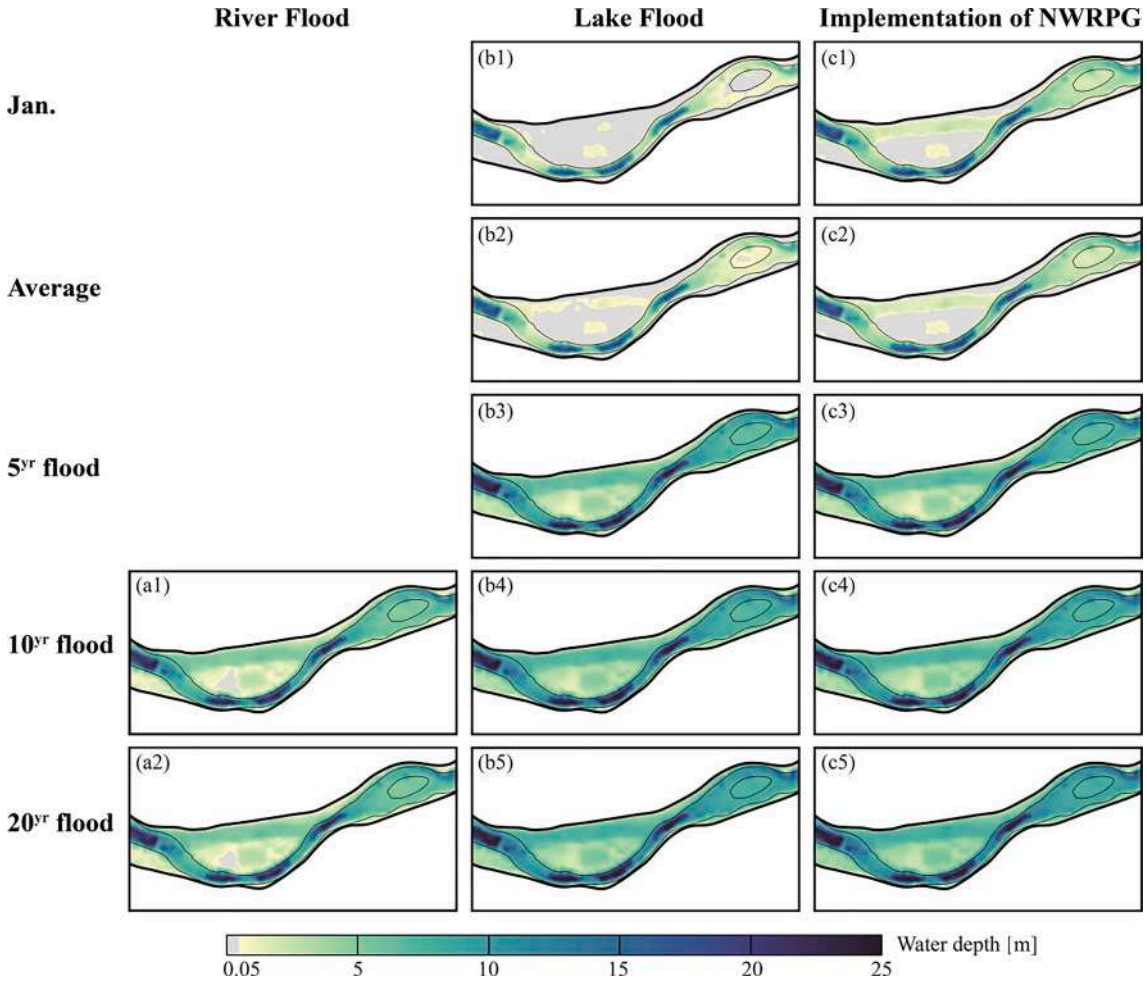

Fig. 5. Water depth under "River Flood", "Lake Flood" and after the implementation of NWRPG. Black outlines represent the outlines of model domain. Thin black solid lines represent the river-floodplain boundaries. Colors represent the water depth.

metrics describe how the river and its floodplain are connected from a Lagrangian point of view.

To test the frequency of particle exchange between the main channel and the floodplain, the distribution of particle residence time (RT) and particle transport distance (PTD) on the left upstream floodplain (Fig. 1 d) was calculated. Since the river-floodplain exchange flux at the left upstream floodplain is small in the January scenarios and at the average annual flow scenarios (Fig. 7), only the flood inundation scenarios are considered here. In the subsequent statistical analysis, only particles that first entered and then left the floodplain were considered, which means that those became stuck in the dry floodplains were excluded. Each particle calculated in the following analysis was weighted by the original water depth at the location where it was emitted to reflect the water column's properties.

The distributions of RT for 5-year, 10-year, and 20-year flood events are presented in Fig. 9. The RTs for the different flood events follow an approximately skewed right distribution. As the flow rate increases in "Lake Flood", the particle average residence time (MRT) decreases. For instance, MRT decreased from 3,176 s at a 5-year flood to 2,933 s at a 20-year flood. The standard deviation (SD) of RT also decreases significantly with increasing flow, indicating an increase in the "uniformity" of water mass movement under large floods. Due to the larger velocity of "River Flood" scenarios, their MRTs are smaller than those of "Lake Flood" scenarios, and the SDs are smaller as well. The "River Flood" scenarios for 10-year and 20-year have similar RT distributions, with MRTs of 1933 s and 1907 s as well as SDs of 433 s and 510 s, respectively. The implementation of NWRPG results in greater velocity. The particles moving with the water body show smaller MRTs and more uniform velocities, as well as lower RT SDs.

The distribution of PTD for 5-year, 10-year, and 20-year flood events is presented in Fig. 10. The PTDs for the different flood events approximately follow the normal distribution closer than the RTs. In "Lake Flood" scenarios, as the discharge increased, the flow path became straight (Fig. 8 b3-5), and the particle travel distance decreased (Fig. 10 b1-3). In "River Flood" scenarios, the PTD was larger than that of "Lake Flood" scenarios, but the SD was smaller. Like RT, "River Flood" scenarios for 10-yr and 20-yr showed close PTD distributions, which may be due to the fact that the floodplains are still not fully inundated, and the different "River Flood" scenarios have similar flow structures. The mean PTD after the implementation of NWRPG and for "Lake Flood" scenarios under different floods did not differ significantly. The implementation of NWRPG results in a slight SD increase in PTD. Although the implementation of the NWRPG accelerated the velocity, the particle flow path was as straight as for the "Lake Flood" scenarios, resulting in a PTD distribution like that of the "Lake Flood" scenarios.

4. Discussion

4.1. Projected effects of NWRPG implementation

Flood pulses are a major driver of improved habitat heterogeneity and diversity in floodplain hydrologic connectivity (Junk et al., 1989). Systematic assessment of the effects of hydrodynamic conditions and water resources management projects on river-floodplain hydrologic

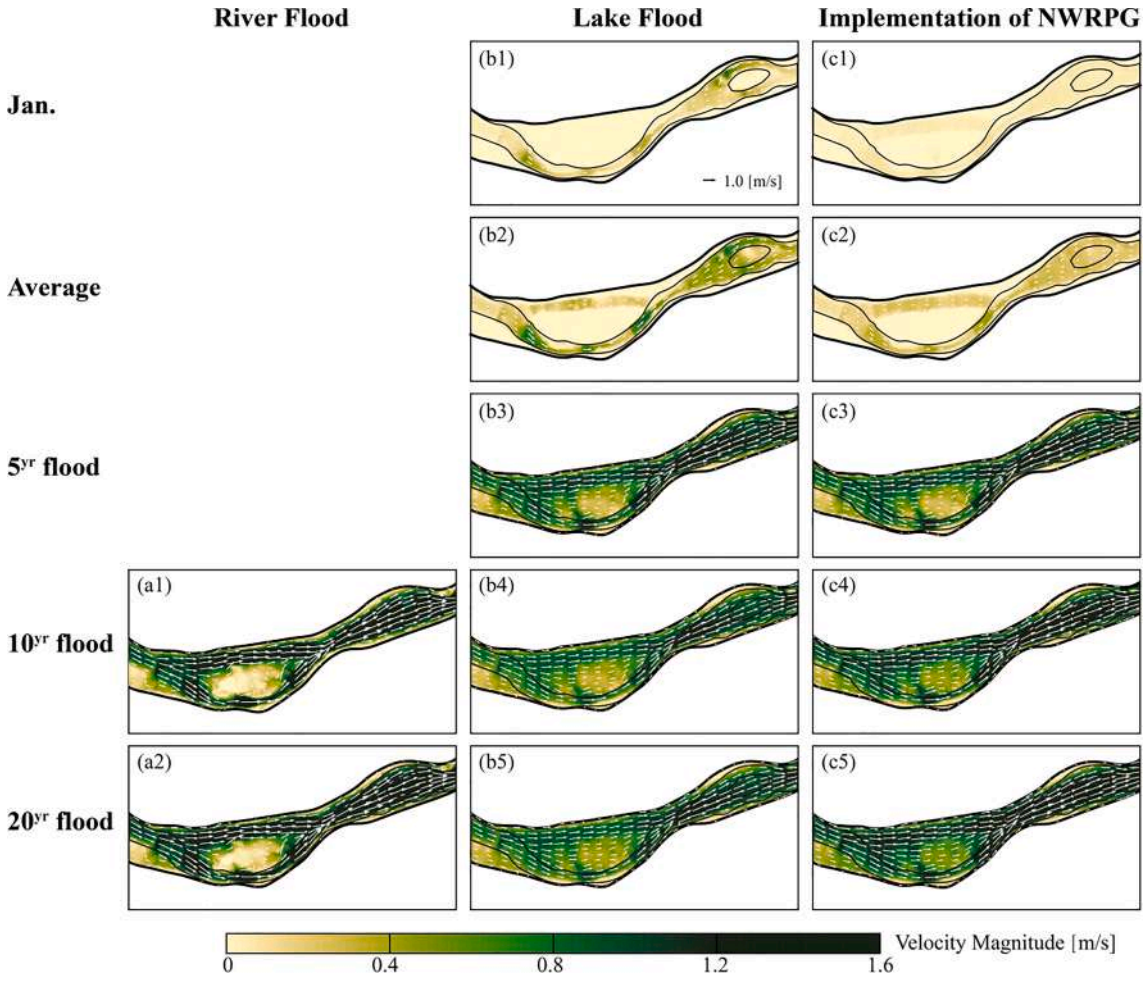

Fig. 6. Depth averaged velocity under "River Flood", "Lake Flood" and after the implementation of NWRPG. Colors represent the velocity magnitude and vectors represent the velocity magnitude and the direction.

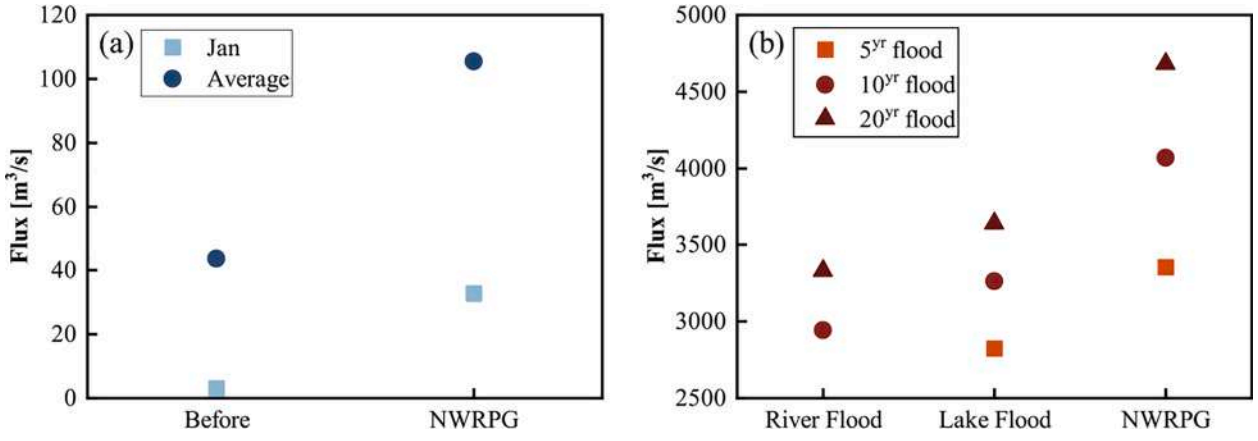

Fig. 7. The transboundary flux of left upstream floodplain of (a) average January discharge and average annual discharge, and (b) different frequencies flood of River Flood, Lake Flood and the implementation of NWRPG.

connectivity is beneficial for understanding and improving the biodiversity of aquatic plants and animals. In this study, we found that the larger floods and the implementation of the NWRPG brought greater streamwise discharge to the floodplain. This is expected to change the habitat heterogeneity of the floodplain. "Lake Flood" corresponds to elevated water levels, which enhances lateral connectivity during floods but reduces potential biological refuges, which is further exacerbated by the implementation of the NWRPG. Regular flood events can effectively enhance the intensity of nutrient and organic matter exchange between the main channel and the floodplain, and the connectivity of low-lying water bodies in the floodplain to the main stem is positively correlated with species abundance. Mouw et al. (2009) found that floodplain water and river water often interact and together serve as a river corridor where many invertebrates live (Mouw et al., 2009).

Table 3
The ratios of the left upstream floodplain transboundary fluxes and the upstream discharges.

	River Flood		Lake Flood		Implementation of NWRPG	
	Ratio [-]	Upstream Discharges[m^3/s]	Ratio [-]	Upstream Discharges[m^3/s]	Ratio [-]	Upstream Discharges [m^3/s]
January	–	–	2.07 %	151.97	35.94 %	122
Average	–	–	6.61 %	496.168	24.11 %	438
5 yr Flood	–	–	67.98 %	4338.68	65.05 %	5122.36
10 yr Flood	57.66 %	4898.08	66.67 %	4898.08	60.32 %	6037.04
20 yr Flood	62.84 %	5338.53	76.29 %	5338.53	68.61 %	6824.79

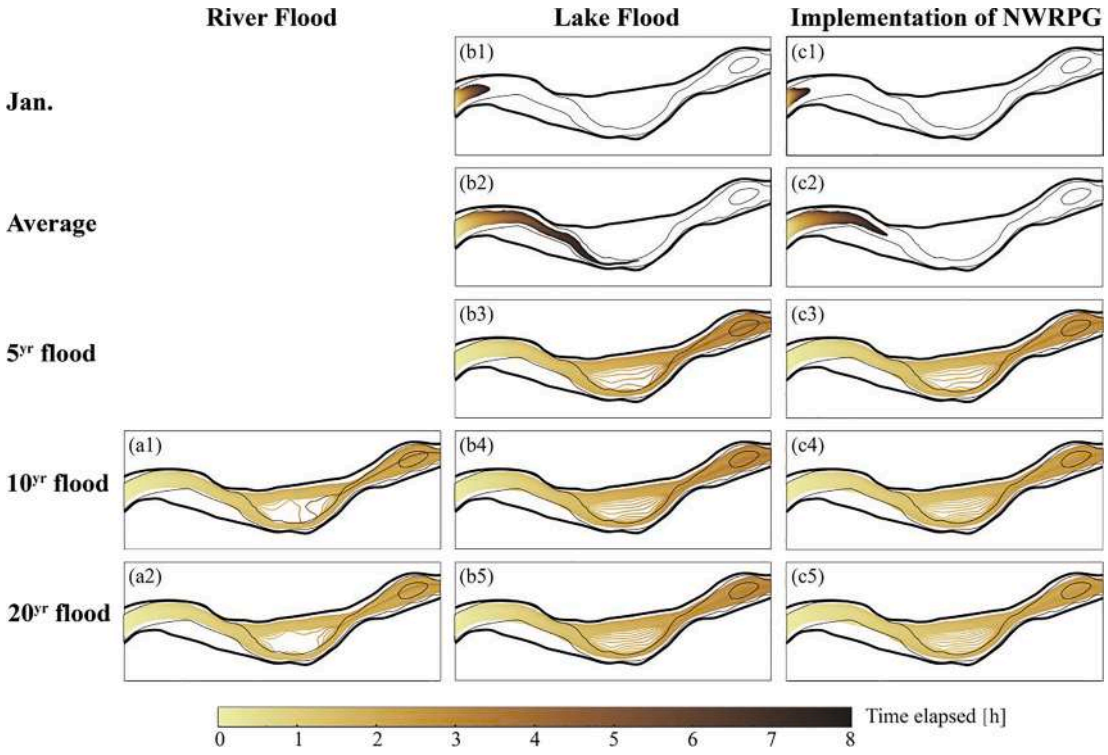

Fig. 8. Particle trajectories. For visual clarity, only 40 particles were illustrated here. Colors of the lines represent the time elapsed.

The implementation of the NWRPG also results in the permanent inundation of portions of the floodplain that would otherwise be exposed during the dry season in January, which can also significantly alter local habitats. Previous studies (Yi et al., 2017) indicated that the implementation of the water resources management projects changed the hydrological condition of the river; the flow in the upstream (reservoir) area slows significantly, even to zero, resulting in sediment deposition, and increases in phytoplankton and zooplankton. When evaluating barrage structures such as gates, it is generally considered necessary to ensure ecological baseflow to maintain upstream and downstream connectivity, but some of the upstream river floodplains are also permanently submerged. In this case, as floodplains are permanently submerged, some biogeochemical reactions cannot occur and the habitat for some organisms is missing. However, the aquatic environment can be maintained due to the elevated water level in the dry season. During the dry season, NWRPG tends to interfere with the natural flow of water in upstream streams. This may be good for the riverine environment in terms of increasing connectivity.

4.2. Effects of natural and engineered hydraulic conditions on river-floodplain connectivity

The interactions between the river and the floodplain in a meandering compound channel are considered here. The main channel-floodplain exchange flux in the meandering compound channel is more from the upstream river, midstream floodplain, and downstream river connectivity due to the straight flow path (Fig. 11). This implies a more intense and complex exchange between the main channel and the floodplain in the meandering river section. The exchange during flooding is actually the upstream–downstream connectivity that maintains the river-floodplain connectivity. This type of river morphology may serve many functions, such as biogeochemical filters and the creation of favorable conditions for organisms (Matheus Carnevali et al., 2021). However, artificial management of rivers, such as channel straightening and extensive construction of embankments, often diminishes the strength of water exchange dynamics and hydrological connectivity, leading to lower levels of biodiversity. Modern river management has tried to restore lateral connectivity (Bolland et al., 2012), but our work proves that it is also important to pay attention to the main channel-floodplain longitudinal connectivity (Fig. 11) in meandering channels during floods.

4.3. Limitations and future developments of this study

There are limitations to this study. The 2D approach for both the hydrodynamic and the particle tracking models is less accurate than 3D models in describing areas with large changes in riverbed elevation. A 3D hydrodynamic model and particle tracking analysis should be carried out to obtain a more detailed picture of the river-floodplain connectivity in the surface and bottom layers. The flood-driven submerged flow

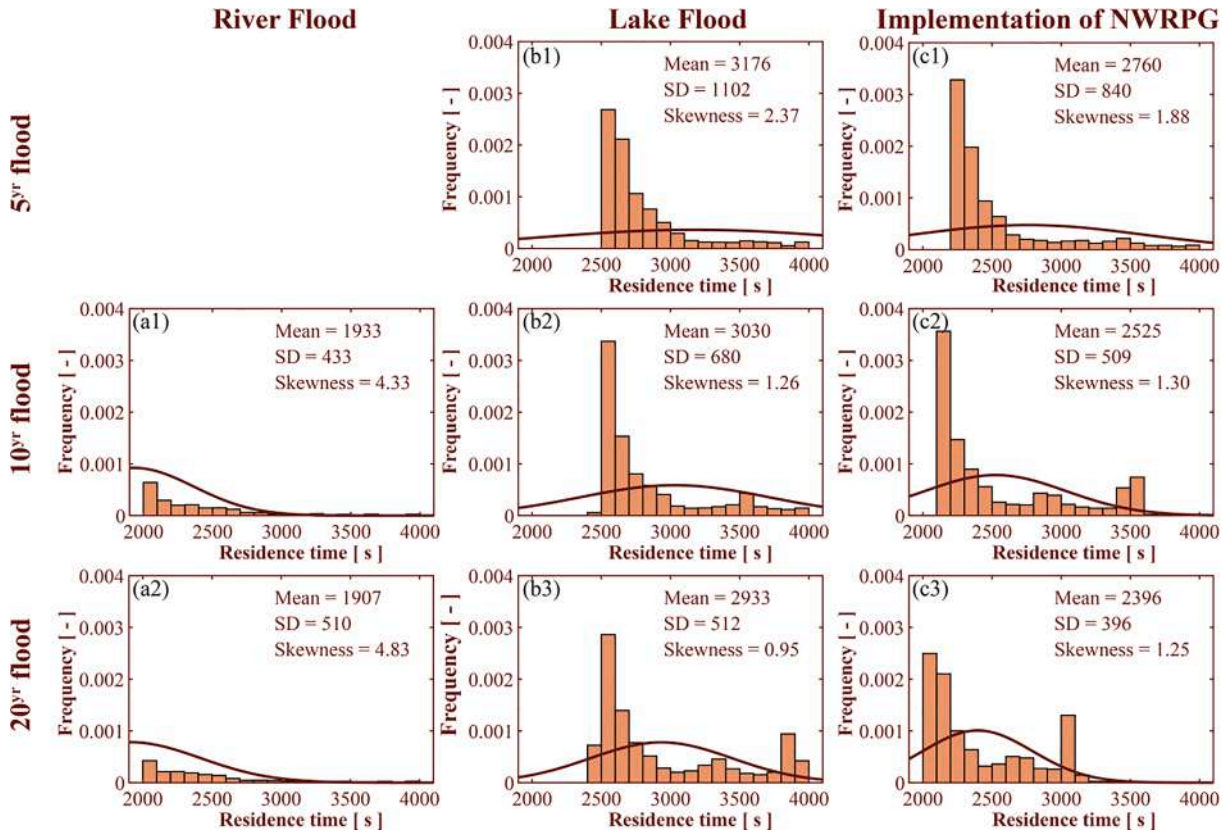

Fig. 9. Histogram of particle residence time (RT) under different floods of 5-year, 10-year and 20-year frequency.

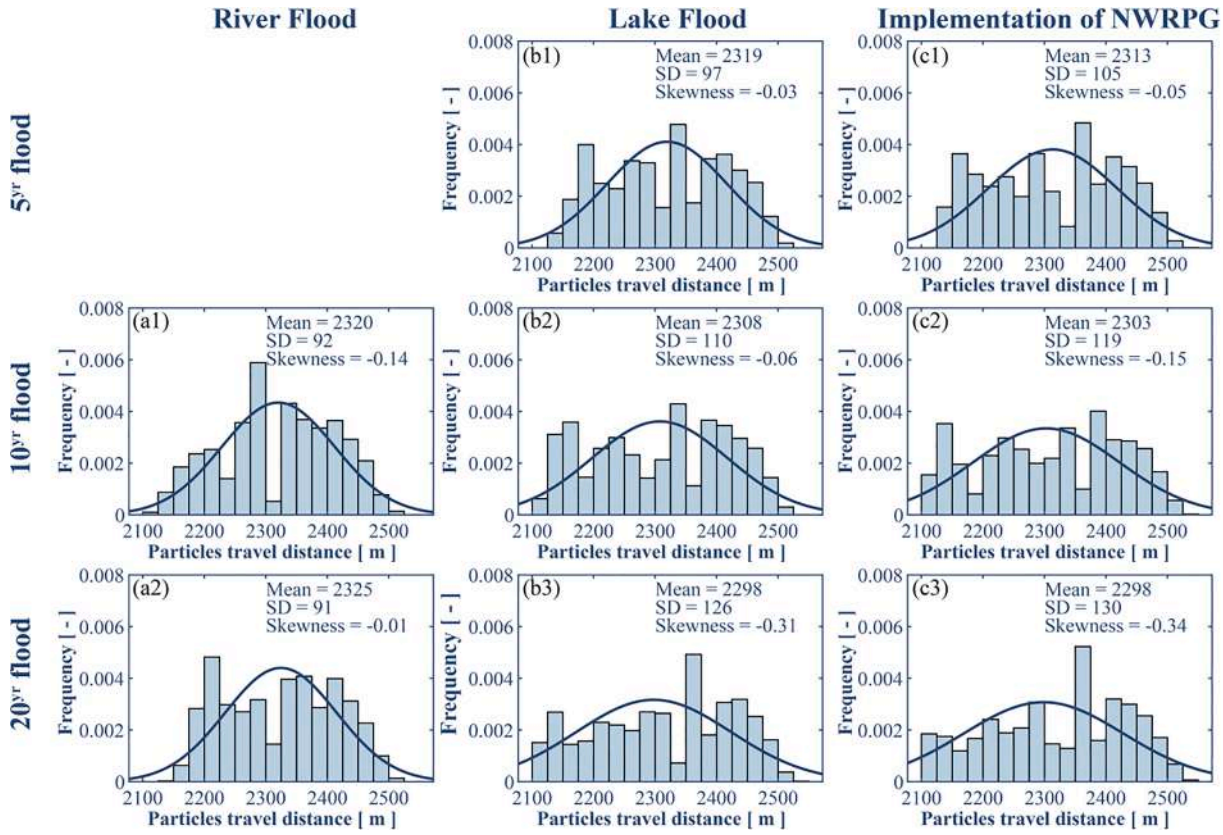

Fig. 10. Histogram of particle travel distance (PTD) under different floods of 5-year, 10-year and 20-year frequency.

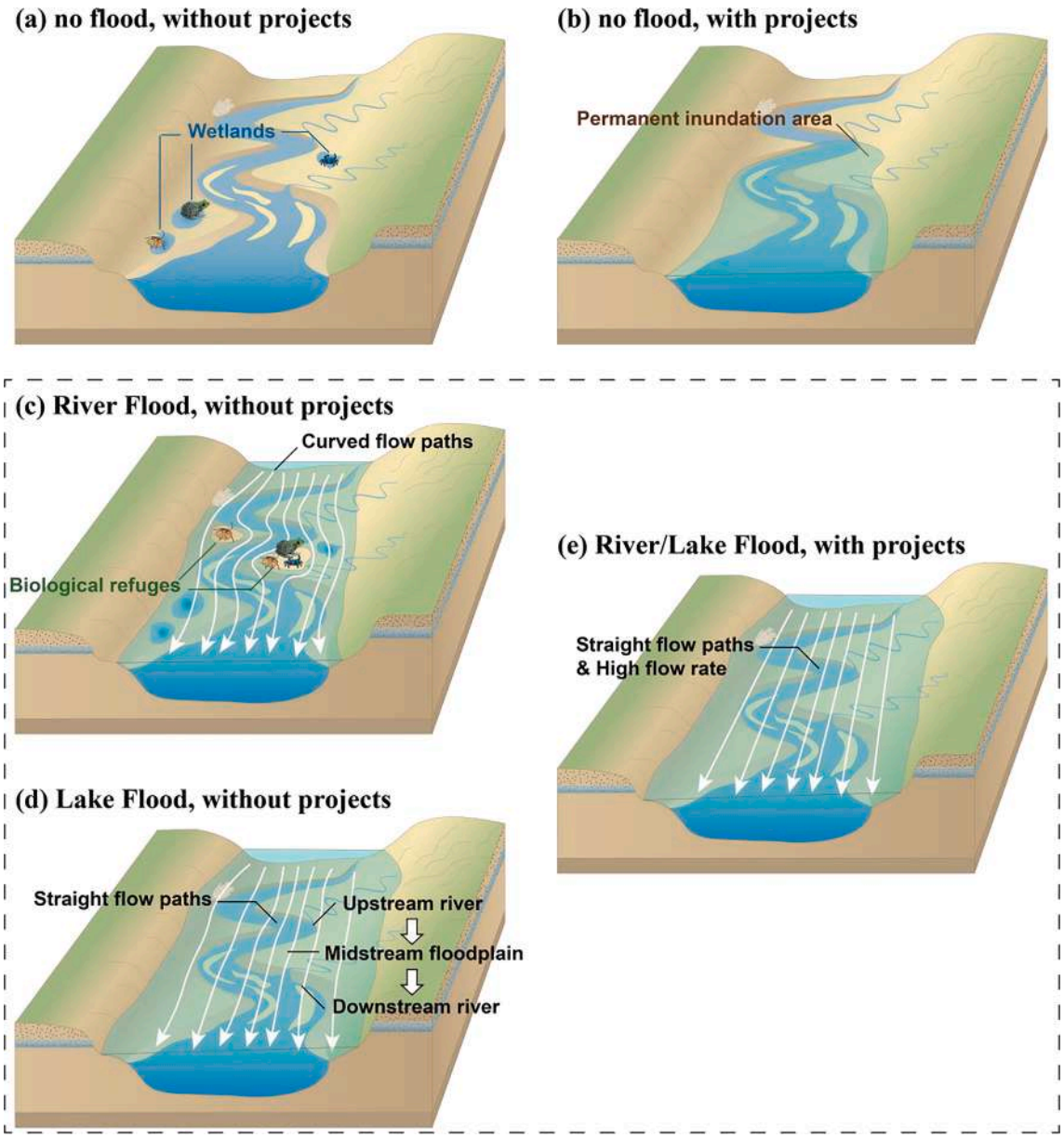

Fig. 11. Sketch of the interactions between river and floodplains in meandering rivers under (a) dry season, (b) dry season after projects, (c) River Flood, and (d) flood after project (similar to Lake Flood).

exchange processes in the river-floodplain system also need to be further explored. In addition, the unsteady flow condition was not considered. The assessment of river-floodplain connectivity and the related material exchange during the unsteady process of flood rising and fall still needs further research. The NWRPG is still in a planning stage, in which it is difficult to consider the unsteady flow. A post-evaluation analysis could be carried out after the implementation of the NWRPG.

The study river reach is part of the Ganjiang Rive which feeds into the Poyang Lake, which is the largest freshwater lake in the Yangtze River Basin and even in China. Poyang Lake can be regarded as a compound river system, which is a river in the dry season and a lake in the flood season (Yuan et al., 2022; Yuan et al., 2021). After the implementation of the Three Gorges Project, the hydrological cycle in the middle and lower reaches of the Yangtze River underwent a dramatic change (Fu et al., 2010; Xu et al., 2013). The sediment concentration was sharply reduced (Yang et al., 2014), the undercutting of clear water and other problems were initially highlighted (Zheng, 2016), and many riverbanks collapsed (Chen et al., 2018). The Poyang Lake Hub Project (PLHP) is planned to be implemented in the Poyang Lake Basin (Wu et al., 2019). This is a major project that focuses on protecting water resources as well as the lake's ecological quality and navigation. The impact of the new hydrological cycle due to PLHP and NWRPG on the whole Poyang Lake basin still needs to be carefully assessed, even considering the effect from the Three Gorges. The PLHP and other projects will increase the water level in the dry season, and the assessment of the river-floodplain connectivity and its impact on biogeochemistry still needs to be studied (Yao et al., 2019).

5. Conclusions

River channel-floodplain hydrological connectivity during floods has an important role in flood control and river habitat assessment. Hydraulic projects often have a negative impact on hydrological connectivity. Several steady flow conditions are considered in the study. Changes in river hydrodynamics and particle motion due to the implementation of the NWRPG as well as to "River Flood" and "Lake Flood"

conditions were comparatively analyzed. Compared to the "River Flood" scenarios, during the "Lake Flood" scenarios the water level and inundated areas were larger, whereas velocity decreased and the residence time (RT) of particles increased. The particle travel distance (PTD) during the "River Flood" scenarios was larger than during the "Lake Flood" scenarios. The larger the flood, the greater the transboundary flux between the river and the floodplain, and the shorter the RT and PTD. The implementation of the NWRPG resulted in the permanent inundation of part of the river floodplain, causing some habitat loss. Due to the increase in discharge, those projects will reduce the RT and cause a smaller SD of RT, with little effect on the PTD distribution.

This study has improved the understanding of the river-floodplain connectivity and provided technical guidance for the assessment of upstream hydrologic connectivity. Research on river-floodplain connectivity and restoration methods that consider the effects of water resources management projects should continue as human use of river systems increases and standards for ecological restoration of rivers become more demanding.

CRediT authorship contribution statement

Yang Xiao: Conceptualization, Methodology, Writing – review & editing, Funding acquisition. **Jiaming Liu:** Methodology, Data curation, Writing – review & editing. **Carlo Gualtieri:** Methodology, Writing – review & editing. **Jun Fu:** Formal analysis. **Ran Gu:** Methodology, Formal analysis, Validation. **Zixuan Wang:** Methodology, Validation. **Taotao Zhang:** Methodology. **Jian Zhou:** Methodology, Formal analysis, Supervision.

Declaration of Competing Interest

The authors declare that they have no known competing financial interests or personal relationships that could have appeared to influence the work reported in this paper.

Data availability

Data will be made available on request.

Acknowledgements

This research was funded by the National Natural Science Foundation of China (Grant number U2240209), the Natural Science Foundation of Jiangsu Province (Grant number BK20191299), the Water Conservancy Science and Technology Project of Jiangsu Province (Grant number 2021055), the State Key Laboratory of Hydrology-Water Resources and Hydraulic Engineering (Grant number 521013152), and the 111 Project (Grant number B17015). The numerical simulation was supported by High Performance Computing Platform, Hohai University.

References

Bernard, R. S., & Schneider, M. L. (1992). *Depth-averaged numerical modeling for curved channels*.

Blankaert, K., Buschman, F., Wijbenga, J., Schielen, R.M.J., 2006. Redistribution of velocity and bed shear stress in straight and curved open channels by means of a bubble screen. J. Hydraul. Eng. 132 (10), 1076–1085. https://doi.org/10.1061/(ASCE)0733-9429(2008)134:2(184).

Blocken, B., Gualtieri, C., 2012. Ten iterative steps for model development and evaluation applied to computational fluid dynamics for environmental fluid mechanics. Environ. Modell. Software 33, 1–22. https://doi.org/10.1016/j.envsoft.2012.02.001.

Bolland, J., Nunn, A., Lucas, M., Cowx, I., 2012. The importance of variable lateral connectivity between artificial floodplain waterbodies and river channels. River Res. Appl. 28 (8), 1189–1199. https://doi.org/10.1002/rra.1498.

Cao, H., Yuan, S., Tang, H., & Lee, J. H.-w. (2020, October 11). Benchmark tests for hydrodynamic simulation of coastal waters using Delft3D-FM. The 30th International Ocean and Polar Engineering Conference.

Chen, X., Chen, L., Stone, M.C., Acharya, K., 2020. Assessing connectivity between the river channel and floodplains during high flows using hydrodynamic modeling and particle tracking analysis. J. Hydrol. 583, 124609 https://doi.org/10.1016/j.jhydrol.2020.124609.

Chen, J., Fang, X., Wen, Z., Chen, Q., Ma, M., Huang, Y., Wu, S., Yang, L.E., 2018. Spatio-temporal patterns and impacts of sediment variations in downstream of the three gorges dam on the yangtze river, China. Sustainability 10 (11), 4093. https://doi.org/10.3390/su10114093.

Covino, T., 2017. Hydrologic connectivity as a framework for understanding biogeochemical flux through watersheds and along fluvial networks [Article]. Geomorphology 277, 133–144. https://doi.org/10.1016/j.geomorph.2016.09.030.

Defne, Z., Ganju, N.K., 2015. Quantifying the residence time and flushing characteristics of a shallow, back-barrier estuary: Application of hydrodynamic and particle tracking models. Estuaries Coasts 38 (5), 1719–1734. https://doi.org/10.1007/s12237-014-9885-3.

Ding, S.-W., Zeng, C., Zhou, J., Wang, L.-L., Chen, C., 2022. Impact of depth ratio on flow structure and turbulence characteristics of compound open channel flows. Water Sci. Eng. 15 (3), 265–272.

Dupuis, V., Proust, S., Berni, C., Paquier, A., 2017. Mixing layer development in compound channel flows with submerged and emergent rigid vegetation over the floodplains. Exp. Fluids 58 (4), 30. https://doi.org/10.1007/s00348-017-2319-9.

Fu, B., Horsburgh, J. S., Jakeman, A. J., Gualtieri, C., Arnold, T., Marshall, L., Green, T. R., Quinn, N. W. T., Volk, M., Hunt, R. J., Vezzaro, L., Croke, B. F. W., Jakeman, J. D., Snow, V., & Rashleigh, B. (2020). Modeling Water Quality in Watersheds: From Here to the Next Generation. *Water Resources Research*, *56*(11), e2020WR027721. https://doi.org/https://doi.org/10.1029/2020WR027721.

Fu, B.-J., Wu, B.-F., Lü, Y.-H., Xu, Z.-H., Cao, J.-H., Niu, D., Yang, G.-S., Zhou, Y.-M., 2010. Three Gorges Project: efforts and challenges for the environment. Prog. Phys. Geogr. 34 (6), 741–754. https://doi.org/10.1177/0309133310370286.

Goeury, C. (2012). *Modélisation du transport des nappes d'hydrocarbures en zone continentale et estuarienne* [Doctor, Université Paris-Est]. France.

Gooseff, M.N., Wlostowski, A., McKnight, D.M., Jaros, C., 2017. Hydrologic connectivity and implications for ecosystem processes - Lessons from naked watersheds [Article]. Geomorphology 277, 63–71. https://doi.org/10.1016/j.geomorph.2016.04.024.

Harvey, J., Gooseff, M., 2015. River corridor science: Hydrologic exchange and ecological consequences from bedforms to basins. Water Resour. Res. 51 (9), 6893–6922. https://doi.org/10.1002/2015WR017617.

He, W., Zhang, J., Yu, X., Chen, S., Luo, J., 2018. Effect of runoff variability and sea level on saltwater intrusion: a case study of nandu river estuary China. Water Resour. Res. 54 (12), 9919–9934. https://doi.org/10.1029/2018WR023285.

Hervouet, J.-M., 2007. Hydrodynamics of free surface flows: modelling with the finite element method. John Wiley & Sons.

Jing, M., Kumar, R., Attinger, S., Li, Q., Lu, C., Hesse, F., 2021. Assessing the contribution of groundwater to catchment travel time distributions through integrating conceptual flux tracking with explicit Lagrangian particle tracking. Adv. Water Resour. 149, 103849 https://doi.org/10.1016/j.advwatres.2021.103849.

Joly, A. (2011). *Modelling of the transport of algae in a coastal environment using a stochastic method* [Doctor, Université Paris-Est]. France.

Junk, W.J., Bayley, P.B., Sparks, R.E., 1989. The flood pulse concept in river-floodplain systems. Can. Spec. Publ. Fish. Aquat. Sci. 106 (1), 110–127.

Kang, H., Choi, S.-U., 2005. 3D numerical simulation of compound open-channel flow with vegetated floodplains by reynolds stress model [journal article]. KSCE J. Civ. Eng. 9 (1), 7–11. https://doi.org/10.1007/bf02829092.

Knight, D.W., Demetriou, J.D., 1983. Flood plain and main channel flow interaction. J. Hydraul. Eng. 109 (8), 1073–1092. https://doi.org/10.1061/(ASCE)0733-9429(1983)109:8(1073).

Lai, S., Bessaih, N., Law, P., Ab Ghani, A., Zakaria, N., Mah, D., 2008. Discharge estimation for equatorial natural rivers with overbank flow. Int. J. River Basin Manage. 6, 13–21. https://doi.org/10.1080/15715124.2008.9635333.

Launder, B., Morse, A., Rodi, W., Spalding, D., 1973. Prediction of free shear flows: a comparison of the performance of six turbulence models. Langley Res. Center Free Turbulent Shear Flows, Vol, NASA, p. 1.

Launder, B.E., Spalding, D.B., 1983. The numerical computation of turbulent flows. In: Numerical Prediction of Flow, Heat Transfer, Turbulence and Combustion. Elsevier, pp. 96–116.

Li, Y., Yang, P., Xu, T., Ren, S., Lin, X., Wei, R., Xu, H., 2008. CFD and digital particle tracking to assess flow characteristics in the labyrinth flow path of a drip irrigation emitter. Irrig. Sci. 26 (5), 427–438. https://doi.org/10.1007/s00271-008-0108-1.

Lim, A., Ismail, Z., Jamal, M. H., Ibrahim, Z., & Jumain, M. (2019). Depth-averaged modelling of vegetated meandering compound channel. In H. Yaacob, N. Z. M. Yunus, I. S. Ibrahim, N. Jamaludin, M. H. Abdullah, I. S. Ahmad, D. S. A. Ismail, Q. A. S. Sirat, & U. H. M. Anuar (Eds.), *12th International Civil Engineering Post Graduate Conference* (Vol. 220). https://doi.org/10.1088/1755-1315/220/1/012038.

Liu, W., 2018. The Study on the Effect of the River and Sediment Proccess in the Tail-area in the Lower Reaches of Fu River in GanJiang River under Comprehensive Water System Improvement [Doctor, Xi'an University of Technology]. Xi'an, China.

Mahl, U.H., Tank, J.L., Roley, S.S., Davis, R.T., 2015. Two-stage ditch floodplains enhance n-removal capacity and reduce turbidity and dissolved p in agricultural streams. J. Am. Water Resour. Assoc. 51 (4), 923–940. https://doi.org/10.1111/1752-1688.12340.

Marinone, S., Ulloa, M., Parés-Sierra, A., Lavín, M., Cudney-Bueno, R., 2008. Connectivity in the northern Gulf of California from particle tracking in a three-dimensional numerical model. J. Mar. Syst. 71 (1–2), 149–158. https://doi.org/10.1016/j.jmarsys.2007.06.005.

Matheus Carnevali, P.B., Lavy, A., Thomas, A.D., Crits-Christoph, A., Diamond, S., Méheust, R., Olm, M.R., Sharrar, A., Lei, S., Dong, W., Falco, N., Bouskill, N., Newcomer, M.E., Nico, P., Wainwright, H., Dwivedi, D., Williams, K.H., Hubbard, S., Banfield, J.F., 2021. Meanders as a scaling motif for understanding of floodplain soil

microbiome and biogeochemical potential at the watershed scale. Microbiome 9 (1). https://doi.org/10.1186/s40168-020-00957-z.
Mouw, J.E., Stanford, J.A., Alaback, P.B., 2009. Influences of flooding and hyporheic exchange on floodplain plant richness and productivity. River Res. Appl. 25 (8), 929–945. https://doi.org/10.1002/rra.1196.
Proust, S., Fernandes, J.N., Leal, J.B., Rivière, N., Peltier, Y., 2017. Mixing layer and coherent structures in compound channel flows: effects of transverse flow, velocity ratio, and vertical confinement. Water Resour. Res. 53 (4), 3387–3406. https://doi.org/10.1002/2016WR019873.
Proust, S., Nikora, V.I., 2020. Compound open-channel flows: effects of transverse currents on the flow structure. J. Fluid Mech. 885, A24. https://doi.org/10.1017/jfm.2019.973.
Rastogi, A.K., Rodi, W., 1978. Predictions of heat and mass transfer in open channels. J. Hydraul. Divis. 104 (3), 397–420. https://doi.org/10.1061/JYCEAJ.0004962.
Rodi, W. (1972). *The prediction of free turbulent boundary layers by use of a two equation model of turbulence* [Doctor, University of London]. London.
Rowiński, P., Radecki-Pawlik, A., 2015. Rivers-Physical. Springer, Fluvial and Environmental Processes.
Salamon, P., Fernàndez-Garcia, D., Gómez-Hernández, J.J., 2006. A review and numerical assessment of the random walk particle tracking method. J. Contam. Hydrol. 87 (3–4), 277–305. https://doi.org/10.1016/j.jconhyd.2006.05.005.
Shiono, K., Knight, D.W., 1991. Turbulent open-channel flows with variable depth across the channel. J. Fluid Mech. 222, 617–646. https://doi.org/10.1017/S0022112091001246.
Shuai, P., Cardenas, M.B., Knappett, P.S.K., Bennett, P.C., Neilson, B.T., 2017. Denitrification in the banks of fluctuating rivers: the effects of river stage amplitude, sediment hydraulic conductivity and dispersivity, and ambient groundwater flow [Article]. Water Resour. Res. 53 (9), 7951–7967. https://doi.org/10.1002/2017wr020610.
Tan, Z., Li, Y., Zhang, Q., Liu, X., Song, Y., Xue, C., Lu, J., 2021. Assessing effective hydrological connectivity for floodplains with a framework integrating habitat suitability and sediment suspension behavior. Water Res. 201, 117253 https://doi.org/10.1016/j.watres.2021.117253.
Tang, H., Cao, H., Yuan, S., Xiao, Y., Jiang, C., Gualtieri, C., 2020. A numerical study of hydrodynamic processes and flood mitigation in a large river-lake system. Water Resour. Manage. 34 (12), 3739–3760. https://doi.org/10.1007/s11269-020-02628-y.
Wang, D., & Tassi, P. (2014, 15th-17th October). Secondary flow corrections into the telemac-mascaret modelling system. Proceedings of the 21st TELEMAC-MASCARET User Conference, Grenoble, France.
Wang, N., Zhang, C., Xiao, Y., Jin, G., Li, L., 2018. Transverse hyporheic flow in the cross-section of a compound river system. Adv. Water Resour. 122, 263–277. https://doi.org/10.1016/j.advwatres.2018.10.006.
Wu, Y., Guo, L., Xia, Z., Jing, P., Chunyu, X., 2019. Reviewing the Poyang lake hydraulic project based on humans' changing cognition of water conservancy projects. Sustainability 11 (9), 2605. https://doi.org/10.3390/su11092605.
Xiao, Y., & Wang, Z. (2007). Flow visualization experiments on horizontal coherent structure in compound channel flow with 45° interface geometry. Proceedings of the congress-international association for hydraulic research, Venice.
Xiao, Y., Wang, Z., Zhang, T., Liang, D., Gu, R., Yuan, K., 2022. TELEMAC modelling of the influence of the Poyang Lake Hydraulic Project on the habitat of Vallisneria natans. Sci. Rep. 12 (1), 1–12. https://doi.org/10.1038/s41598-022-11314-5.
Xu, X., Tan, Y., Yang, G., 2013. Environmental impact assessments of the Three Gorges Project in China: Issues and interventions. Earth Sci. Rev. 124, 115–125. https://doi.org/10.1016/j.earscirev.2013.05.007.
Yang, S., Milliman, J., Xu, K., Deng, B., Zhang, X., Luo, X., 2014. Downstream sedimentary and geomorphic impacts of the three gorges dam on the Yangtze River. Earth Sci. Rev. 138, 469–486. https://doi.org/10.1016/j.earscirev.2014.07.006.
Yao, S., Li, X., Liu, C., Yuan, D., Zhu, L., Ma, X., Yu, J., Wang, G., Kuang, W., 2019. Quantitative assessment of impact of the proposed Poyang Lake Hydraulic Project (China) on the habitat suitability of migratory birds. Water 11 (8), 1639. https://doi.org/10.3390/w11081639.
Yi, Y., Cheng, X., Yang, Z., Wieprecht, S., Zhang, S., Wu, Y., 2017. Evaluating the ecological influence of hydraulic projects: A review of aquatic habitat suitability models. Renew. Sustain. Energy Rev. 68, 748–762. https://doi.org/10.1016/j.rser.2016.09.138.
Yuan, S., Tang, H., Li, K., Xu, L., Xiao, Y., Gualtieri, C., Rennie, C., & Melville, B. (2021). Hydrodynamics, Sediment Transport and Morphological Features at the Confluence Between the Yangtze River and the Poyang Lake. *Water Resources Research*, *57*(3), e2020WR028284. https://doi.org/https://doi.org/10.1029/2020WR028284.
Yuan, S., Xu, L., Tang, H., Xiao, Y., Gualtieri, C., 2022. The dynamics of river confluences and their effects on the ecology of aquatic environment: A review. J Hydrodyn 34, 1–14. https://doi.org/10.1007/s42241-022-0001-z.
Zhao, H., Chen, Q., Walker, N.D., Zheng, Q., MacIntyre, H.L., 2011. A study of sediment transport in a shallow estuary using MODIS imagery and particle tracking simulation. Int. J. Remote Sens. 32 (21), 6653–6671. https://doi.org/10.1080/01431161.2010.512938.
Zheng, S., 2016. Reflections on the three gorges project since its operation. Engineering 2 (4), 389–397. https://doi.org/10.1016/J.ENG.2016.04.002.